Research Article | Vol. 26, No. 2 | 22 Jan 2018 | OPTICS EXPRESS 1443
Optics EXPRESS

Fast optimization method of designing a wideband metasurface without using the Pancharatnam–Berry phase

SAI SUI,[1] HUA MA,[1,*] YUEGUANG LV,[2] JIAFU WANG,[1] ZHIQIANG LI,[1] JIEQIU ZHANG,[1] ZHUO XU,[3] AND SHAOBO QU[1]

[1]*College of Science, Air Force Engineering University, Xi'an, Shaanxi, 710051, China*
[2]*College of Science, Harbin Institute of Technology, Harbin, Heilongjiang, 150001, China*
[3]*School of Electronics & Information Engineering, Xi'an Jiaotong University, Xi'an, Shaanxi, 710049, China*
**mahuar@163.com*

Abstract: Arbitrary control of electromagnetic waves remains a significant challenge although it promises many important applications. Here, we proposed a fast optimization method of designing a wideband metasurface without using the Pancharatnam-Berry (PB) phase, of which the elements are non-absorptive and capable of predicting the wideband and smooth phase-shift. In our design method, the metasurface is composed of low-Q-factor resonant elements without using the PB phase, and is optimized by the genetic algorithm and nonlinear fitting method, having the advantages that the far field scattering patterns can be quickly synthesized by the hybrid array patterns. To validate the design method, a wideband low radar cross section metasurface is demonstrated, showing good feasibility and performance of wideband RCS reduction. This work reveals an opportunity arising from a metasurface in effective manipulation of microwave and flexible fast optimal design method.

OCIS codes: (160.3918) Metamaterials; (050.6624) Subwavelength structures; (290.1990) Diffusion.

References and links

1. N. Yu, P. Genevet, M. A. Kats, F. Aieta, J. P. Tetienne, F. Capasso, and Z. Gaburro, "Light propagation with phase discontinuities: generalized laws of reflection and refraction," Science **334**(6054), 333–337 (2011).
2. S. Sun, K. Y. Yang, C. M. Wang, T. K. Juan, W. T. Chen, C. Y. Liao, Q. He, S. Xiao, W. T. Kung, G. Y. Guo, L. Zhou, and D. P. Tsai, "High-efficiency broadband anomalous reflection by gradient meta-surfaces," Nano Lett. **12**(12), 6223–6229 (2012).
3. C. L. Holloway, E. F. Kuester, J. A. Gordon, J. O'Hara, J. Booth, and D. R. Smith, "An overview of the theory and applications of metasurfaces: the two-dimensional equivalents of metamaterials," IEEE Antennas Propag. Mag. **54**(2), 10–35 (2012).
4. X. Li, S. Xiao, B. Cai, Q. He, T. J. Cui, and L. Zhou, "Flat metasurfaces to focus electromagnetic waves in reflection geometry," Opt. Lett. **37**(23), 4940–4942 (2012).
5. N. Engheta and R. W. Ziolkowski, *Metamaterials: Physics and Engineering Explorations* (John Wiley & Sons, 2006).
6. C. Pfeiffer, N. K. Emani, A. M. Shaltout, A. Boltasseva, V. M. Shalaev, and A. Grbic, "Efficient light bending with isotropic metamaterial Huygens' surfaces," Nano Lett. **14**(5), 2491–2497 (2014).
7. S. Xiao, H. Mühlenbernd, G. Li, M. Kenney, F. Liu, T. Zentgraf, S. Zhang, and J. Li, "Helicity-preserving omnidirectional plasmonic mirror," Adv. Opt. Mater. **4**(5), 654–658 (2016).
8. M. Khorasaninejad, W. T. Chen, R. C. Devlin, J. Oh, A. Y. Zhu, and F. Capasso, "Metalenses at visible wavelengths: diffraction-limited focusing and subwavelength resolution imaging," Science **352**(6290), 1190–1194 (2016).
9. M. Decker, I. Staude, M. Falkner, J. Dominguez, D. N. Neshev, I. Brener, T. Pertsch, and Y. S. Kivshar, "High-efficiency dielectric huygens' surfaces," Adv. Opt. Mater. **3**(6), 813–820 (2015).
10. T. J. Cui, M. Q. Qi, X. Wan, J. Zhao, and Q. Cheng, "Coding metamaterials, digital metamaterials and programmable metamaterials," Light Sci. Appl. **3**(10), e218 (2014).
11. C. Della Giovampaola and N. Engheta, "Digital metamaterials," Nat. Mater. **13**(12), 1115–1121 (2014).
12. T. J. Cui, S. Liu, and L. L. Lian, "Information entropy of coding metasurface," Light Sci. Appl. **5**(11), e16172 (2016).

#307185 https://doi.org/10.1364/OE.26.001443
Journal © 2018 Received 14 Sep 2017; revised 6 Dec 2017; accepted 4 Jan 2018; published 12 Jan 2018

Optics EXPRESS

13. L. H. Gao, Q. Cheng, J. Yang, S. J. Ma, J. Zhao, S. Liu, H. B. Chen, Q. He, W. X. Jiang, H. F. Ma, Q. Y. Wen, L. J. Liang, B. B. Jin, W. W. Liu, L. Zhou, J. Q. Yao, P. H. Wu, and T. J. Cui, "Broadband diffusion of terahertz waves by multi-bit coding metasurfaces," Light Sci. Appl. **4**(9), e324 (2015).
14. D. S. Dong, J. Yang, Q. Cheng, J. Zhao, L. H. Gao, S. J. Ma, S. Liu, H. B. Chen, Q. He, W. W. Liu, Z. Fang, L. Zhou, and T. J. Cui, "Terahertz broadband low-reflection metasurface by controlling phase distributions," Adv. Opt. Mater. **3**(10), 1405–1410 (2015).
15. F. Costa, A. Monorchio, and G. Manara, "Wideband scattering diffusion by using diffraction of periodic surfaces and optimized unit cell geometries," Sci. Rep. **6**(1), 25458 (2016).
16. S. J. Li, X. Y. Cao, L. M. Xu, L. J. Zhou, H. H. Yang, J. F. Han, Z. Zhang, D. Zhang, X. Liu, C. Zhang, Y. J. Zheng, and Y. Zhao, "Ultra-broadband reflective metamaterial with RCS reduction based on polarization convertor, information entropy theory and genetic optimization algorithm," Sci. Rep. **5**(1), 37409 (2016).
17. K. Wang, J. Zhao, Q. Cheng, D. S. Dong, and T. J. Cui, "Broadband and broad-angle low-scattering metasurface based on hybrid optimization algorithm," Sci. Rep. **4**(1), 5935 (2014).
18. Q. Q. Zheng, Y. F. Li, J. Q. Zhang, H. Ma, J. F. Wang, Y. Q. Pang, Y. J. Han, S. Sui, Y. Shen, H. Y. Chen, and S. B. Qu, "Wideband, wide-angle coding phase gradient metasurfaces based on Pancharatnam-Berry phase," Sci. Rep. **7**, 43543 (2017).
19. H. T. Chen, A. J. Taylor, and N. Yu, "A review of metasurfaces: physics and applications," Rep. Prog. Phys. **79**(7), 076401 (2016).
20. M. Paquay, J. C. Iriarte, I. Ederra, R. Gonzalo, and P. de Maagt, "Thin AMC Structure for Radar Cross-Section Reduction," IEEE Trans. Antenn. Propag. **55**(12), 3630–3638 (2007).
21. T. Hao, C. J. Stevens, and D. J. Edwards, "Optimization of metamaterials by Q factor," Electron. Lett. **41**(11), 653–654 (2005).
22. S. Sui, H. Ma, J. F. Wang, M. D. Feng, Y. Q. Pang, S. Xia, Z. Xu, and S. B. Qu, "Symmetry-based coding method and synthesis topology optimization design of ultrawideband polarization conversion metasurfaces," Appl. Phys. Lett. **109**(1), 014104 (2016).
23. C. A. Balanis, *Antenna Theory: Analysis and Design*, 3rd ed. (Wiley, 2005).

1. Introduction

Metasurfaces are periodic two-dimensional planar arrays of sub-wavelength elements. Recently, it has been obtaining great popularity both in academic and engineering field owing to its extraordinary capability that cannot be normally found in nature, such as, flexible control of polarization state, direction of propagation and amplitude of electromagnetic [1–9]. More recently, coding metasurfaces have received increasing attention because of its potential application in imaging, scattering pattern control and information communication [10–14]. Since Yu et al. proposed and achieved the phase gradient metasurfaces on the basis of generalized versions of reflection and refraction law (general Snell's law), in general, both design of metasurfaces and coding metasurfaces are depended on phase discontinuity elements. However, metasurface developed so far encounter an intrinsic contradiction between extending the bandwidth and improving working efficiency. With the extensive investigation in the past decades, various types of metasurfaces, such as multiple independent resonances, coupled antenna resonances, and geometric effects, have been developed and widely applied to extend the phase response to cover the entire 2π range [15–18]. Among them, an approach to introducing entire 2π phase discontinuity is to use the so-called Pancharatnam-Berry (PB) phase by using anisotropic, subwavelength scatters with identical geometric parameters but spatially varying orientations [19]. However, this approach is associated with polarization change, which limits the maneuverability of application.

Up to now, more and more research efforts have been devoting to extend working-band of metasurface both in microwave and terahertz spectrum, where many complicated geometries and optimization methods have been introduced. The most common method is to choose and design complicated geometries with multi-resonances, which are used to broaden the bandwidth in accordance with time-consuming full wave simulation and parameters sweep. Both experientialism and intuition inspiring measures are out of efficiency. Here, we proposed a fast optimization method of designing wideband metasurface without using PB phase. Synthetical analysis and optimal design of low Q-factor elements are demonstrated for various phase-response element design. Furthermore, to achieve fast and optimal design, nonlinear fitting method and both binary and real number coding genetic algorithm are used.

Optics EXPRESS

As a verification, a broadband coding metasurface capable of far-field scattering pattern manipulation and radar cross section reduction is demonstrated. The simplified prototype of coding metasurface was implemented by a chessboard-like surface composed of a series of perfect electric-conductor (PEC) elements and artificial magnetic-conductor (AMC) elements with π reflected phase-difference [20]. Based on the concept, the coding sequences of "0" and "1" are analogized to the PEC-like and AMC-like elements, so various functionalities can be achieved such as anomalous reflection and diffusion. The coding metasurfaces design contain two main step: one is to design and choose proper coding elements with opposite phase in wideband range. The other is the optimization procedure of array coding sequence. Based on proper design of coding sequence, the coding metasurface can successfully disperses the scattering energy into several desire-off-normal directions.

In this work, the key problems of non-absorption metasurface design are various phase-response elements design and its arrangement. Synthetical analysis and optimal design of low Q-factor elements are demonstrated for various phase-response element design. In order to achieve fast and optimal design procedure, two measures are employed in this paper: one is to choose element with low Q-factor, leading to smooth and wideband phase variation. The other is the fast optimization synthesis of coding element and array coding sequence, which can greatly reduce the burden of the computation time and memory sources. To validate the design criterions, a low radar cross section (RCS) metasurface is designed and experimentally characterized. Good agreements have been achieved between the simulated and measured results, showing the applicability and effectiveness of the proposed method.

2. The Q-factor analysis and nonlinear fitting

The variation of reflection coefficient phase is one of the most important properties of the elements, because the phase varies with frequency while, ideally, the magnitude of the reflection coefficient of a lossless ground plane is unity. In the published papers, the high efficient broadband anomalous reflection can be achieved by utilizing the magnetic resonance between metallic patch and ground plane [21], where the resonance with low Q-factor is benefit for working bandwidth broaden. Here we demonstrate the influence between the phase shift and the Q-factor, using equivalent circuit model analysis.

According to RLC series and parallel resonance circuit, the phase shift of entire unit cell can be expressed as $\theta = arc\tan\left(Q(1-\varpi^2)/\varpi\right)$, where $\varpi = \omega/\omega_0$ is normalized angular frequency. Thus, the connection of Q-factor and phase shift are proposed in Fig. 1. As shown clearly, the higher Q-factor lead to more rapidly phase shift around ω_0, which is not benefit to broaden working bandwidth, and vice-versa. Otherwise, the phase shift can hardly cover the entire 0~360° when the Q-factor is too small. Thus, a proper coding element with low Q-factor should be chosen to smoothly cover the entire 0~360° phase shift.

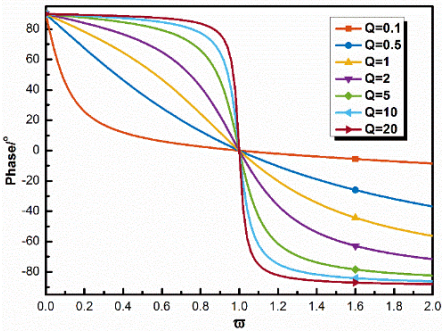

Fig. 1. The frequency dependence between Q-factor and phase shift.

Optics EXPRESS

The unit cell topology of the Crusades is illustrated in Fig. 2(a), where the parameters are $p = 5mm$, $d = 2mm$. By applying the proper geometry design, this unit cell can be modelled as a low Q-factor coding element, demonstrating in Fig. 2(b). In simulation, both upper and under of the metal is copper and the middle dielectric is F4B with relative permittivity of 2.65.

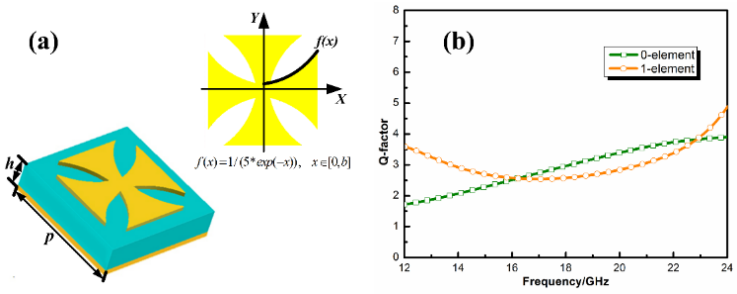

Fig. 2. (a) Schematic of the unit cell topology of the Crusades. (b) The corresponding low Q-factor in wideband by proper design of unit cell.

In previous papers, a number of structures with broadband features have been proposed and discussed in detail. However, most of them are depended on time-consuming simulation of parameter sweep and inefficiently artificial selection. Recently, based on topology optimization design, the optimization method has been used in element determination and optimizing its performance [16, 22]. However, this method need massive full wave simulations and the optimized results are usually sink into local optimal solution. Here, we combine few full wave simulation results and nonlinear fitting method to determine the unit cell geometer. Firstly, a few parameter samples of b are chosen, utilizing CST for full wave simulation, so the S-parameter and reflective phase can be obtained. Next, the connection between parameter and reflective phase can be imitated by using nonlinear fitting. Here, we adopt following equation to fitting limited number of simulated reflective phase result.

$$Phase = P_1 * b(f)^N + P_2 * b(f)^{(N-1)} + ... + P_N * b(f) + P_{N+1} \quad (1)$$

where $Phase$ is reflective phase matrix; $P_1, P_2 ... P_N, P_{N+1}$ are the nonlinear fitting coefficient, and $b(f)$ is column vector of b in various frequencies of f. The fitting and simulated reflective phase is shown clearly in Fig. 3, in which the discrete marker and the continues line represent full wave simulation results and nonlinear fitting results respectively.

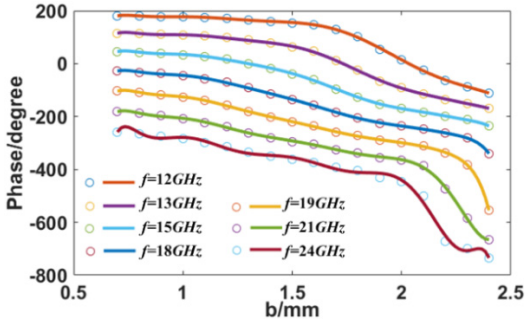

Fig. 3. The relationship between parameter b and its reflective phase utilizing nonlinear fitting with discrete frequency sample of 12, 13, 15, 18, 19, 21, 24GHz respectively.

Optics EXPRESS

3. Fast optimization synthesis of coding element and array coding sequence

To this end, the relationship between the reflective phase and parameter b can be imitated by nonlinear formulation Eq. (1). According to the coding metasurface design demand, 10dB RCS reduction occurs, in the ideal case of an infinite metasurface within $180^\circ \pm 37^\circ$ phase different between "0" and "1" coding elements. To fulfill this purpose, a real number encoding genetic algorithm (GA) is adopted to implement the geometry parameter determination, which optimize the geometry parameter b. The optimization goal is to achieve $180^\circ \pm 37^\circ$ $180^\circ \pm 37^\circ$ phase shift in wideband range and the fitness function, as evaluated function, can be expressed as Eq. (2). The optimization procedure is iterated until the desired fitness result is obtained or maximum iteration condition is reached.

$$fitness1 = \int_{fstart}^{fstop} g(f) \tag{2}$$

$$g(f) = \begin{cases} 1 & if \quad 180^\circ - 37^\circ < \left| phase_{b1}(f) - phase_{b2}(f) \right| < 180^\circ + 37^\circ \\ 0 & else \end{cases} \tag{3}$$

The bigger fitness value the more wideband range of $[fstart, fstop]$, as result, the optimized parameter can be achieved as $b1 = 0.738, b2 = 1.942$. This optimization procedure, using nonlinear fitting method without full wave simulation, can greatly reduce the burden of the computation time and memory source. As a verification, the full wave simulation is carried out and the results are shown in Fig. 4. The reflective phase can achieve about 180-degree shift within 12-24GHz, moreover, the nonlinear fitting method is verified.

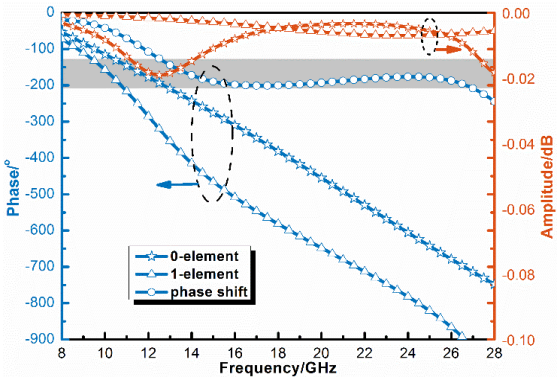

Fig. 4. The simulation result of reflective phase and amplitude of the optimized coding element "0" and "1", which parameter are $b1 = 0.738, b2 = 1.942$ respectively.

Once the coding elements have been prepared, we are going to seek for the optimal array coding sequence, as well as configuration of the diffusion metasurface. The proper array coding sequence can achieve that the scattering energy in all direction can be redirected to minimize directional reflection. According to the array theory [23], with $M \times N$ array composed of opposite reflection phase coding elements, the total scattering far-field of the metasurface can be calculated by $E_{total} = EF \times AF$ where EF is the pattern function of coding element and uniform with non-absorption reflection. AF represents the array factor which can be denoted as Eq. (4).

$$AF = \sum_{m=1}^{M} \sum_{n=1}^{N} exp\{jkd[(m-1/2)\sin\theta\cos\varphi + (n-1/2)\sin\theta\sin\varphi] + j\phi(m,n)\} \tag{4}$$

Optics EXPRESS

where d is the distance between two adjacent array; θ and φ are the elevation and azimuth angles, respectively; $\phi(m,n)$ is the reflective phase of each coding element which are simplified as "0" and "1", so the whole metasurface can be denoted as a $M \times N$ coding matrix.

The $M \times N$ coding matrix can be esteemed as a binary sequence of $M \times N$ length. To obtain low RCS, the GA combining with array factor is utilized again. The difference is that this optimization procedure requires binary coding, which accord with whole metasurface array coding sequence. For the lowest RCS goal, focusing optimization procedure on finding optimal coding sequence, the fitness function can be set as $fitness2 = min(AF_{max})$, where AF_{max} is the maximum value of AF corresponding to given coding matrix. Generally, the bigger the array size, the better RCS reduction performance. In this paper, considering the time consuming and computation burden, the metasurface is discretized with 8×8 coding elements, of which each coding element consists of four unit-cell about λ length.

The flow chart of fast optimization synthesis of coding element and array coding sequence is demonstrated as Fig. 5, of which the whole design procedure is software-automatically. The GA optimization procedure is used twice by coding element optimization and coding sequence optimization. The best and average value of fitness function of coding sequence optimization procedure is shown in Fig. 6, which the iteration terminated after 153 generation, consuming for few minutes, and the optimization procedure converged to a stable solution.

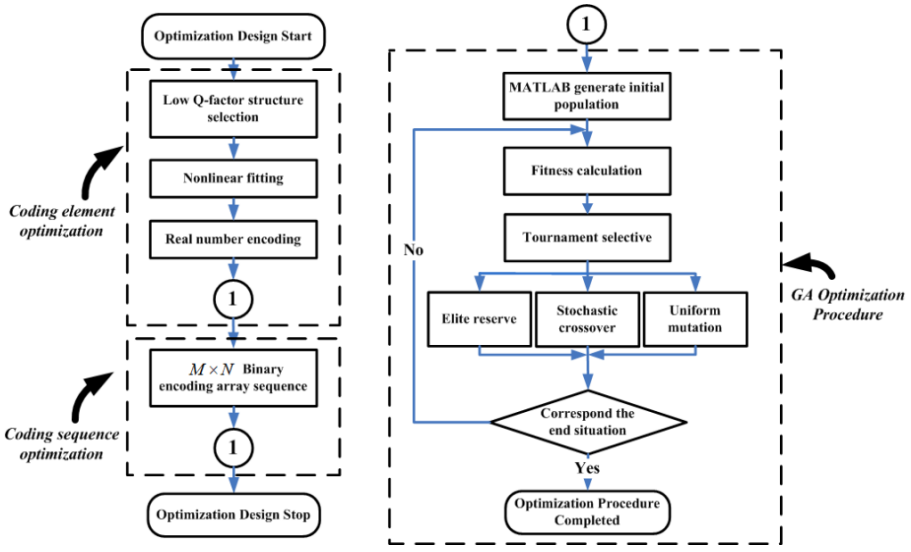

Fig. 5. The flow chart of fast optimization synthesis of coding element and array coding sequence

Optics EXPRESS

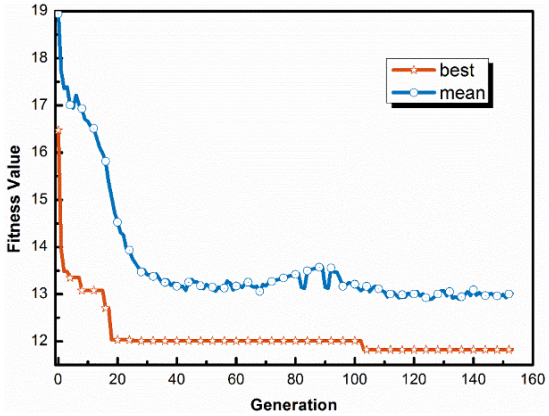

Fig. 6. The evolution plot of array coding sequence optimization procedure.

Once the optimal coding element and coding sequence are prepared, the final coding metasurface can be established and simulated by CST VBA macro, which is used for the automation of common tasks, and the coding element configuration is shown clearly in Fig. 7. The 2D and 3D scattering pattern of central frequency (18GHz) and equal-area-metal are simulated by the full wave electromagnetic software (CST Microwave Studio) by analogy with MATLAB simulation, as shown in Fig. 8, respectively. To obtain wideband RCS reduction performance, the comparison of metal and optimized coding metasurface are simulated and the results are demonstrated as Fig. 9. The 10dBm2 monostatic RCS reduction can be achieved in wide-frequency-band ranging from 12 to 24GHz, which has good agreement with theoretically prediction.

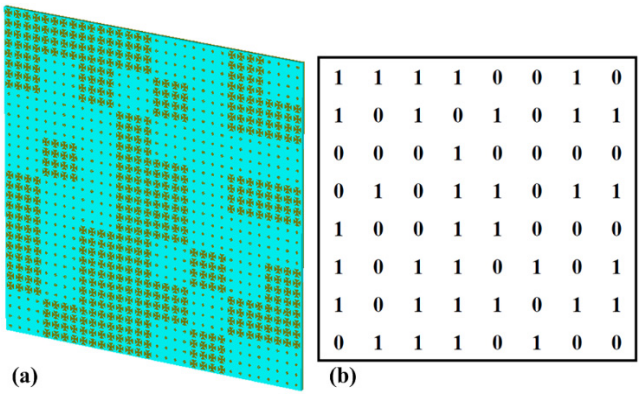

Fig. 7. (a) The optimized configuration of coding metasurface; (b) Corresponding distribution of digital element “0” and “1”.

Optics EXPRESS

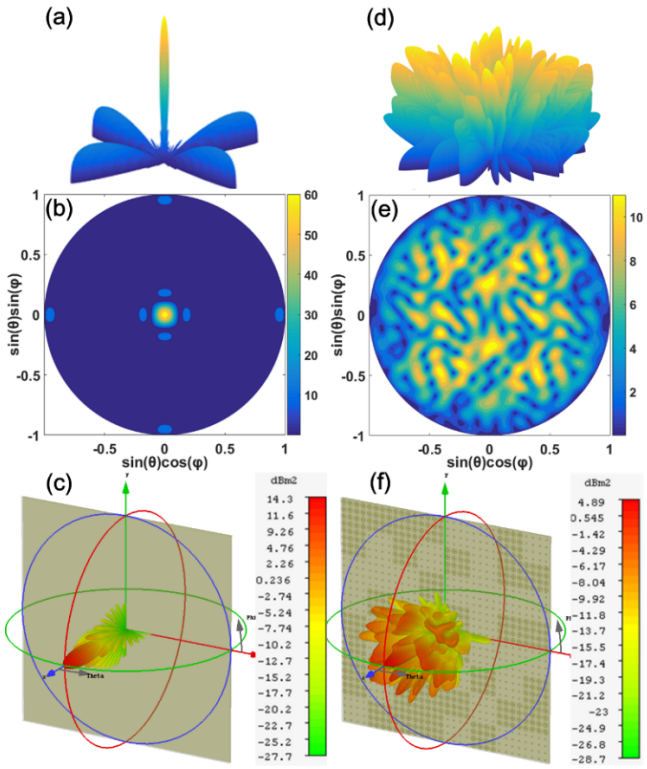

Fig. 8. Schematic of electric-field scattering pattern of metal in 3D (a) and 2D (b); (c) The full wave simulation result; (d) and (e) are schematic of 2D and 3D electric-field scattering pattern of optimized coding metasurface, respectively; (f) The full wave simulation result of optimal coding metasurface.

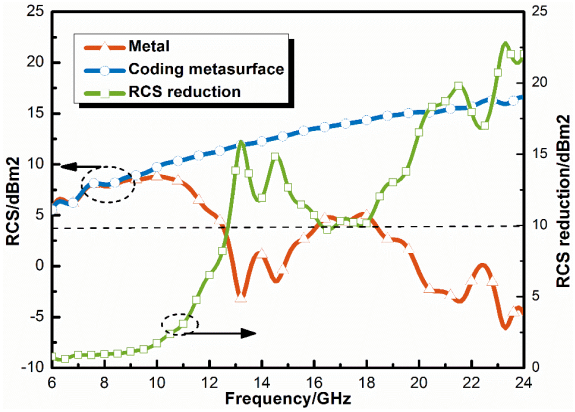

Fig. 9. The RCS reduction of metal and optimized coding metasurface

4. Experiment and discussion

To validate the method, a metasurface is fabricated through photolithography with 8×8 coding element and 160×160mm^2 , and experimental measurements are carried out in a microwave chamber with a pair of broadband horn antennas serving as the transmitter and receiver. The photograph of the fabricated prototype and the measured backward-reflection as a function of frequency are shown in Figs. 10(a) and 10(b), respectively. The experiment

results roughly agreement with the simulation results, which might originate from the drawback of machining accuracy and experimental environment.

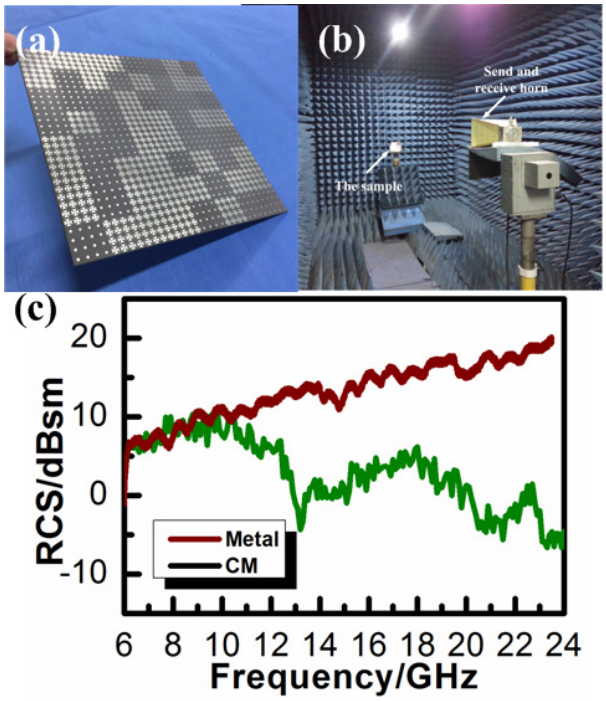

Fig. 10. (a) and (b) Photograph of the fabricated metasurface and measurement environment. (c) The measured backward reflection spectra.

Compared with previous research, this paper chosen a low-Q-factor coding element and combined with nonlinear fitting and fast optimization synthesis of coding element and array coding sequence, where the burden of computation time and memory source are significantly reduced.

5. Conclusion

We have proposed a fast optimization method of designing wideband metasurface without using Pancharatnam-Berry phase, where the computation burden and time consumption is significantly reduced. Two major methods are the crux: the first one is low Q-factor elements analysis and nonlinear fitting to achieve fast calculation of reflective phase, as a function of various geometry parameter; The other one is fast optimization synthesis of coding element and array coding sequence, which has a good potential for application of RCS reduction in wide frequency range. The whole design utilizes twice genetic algorithm of real number encoding and binary encoding, significantly improving the efficiency of the design procedure. Finally, as a verification, an optimal coding metasurface is established and measured. Both simulation and experiment results indicated that the feasibility and the performance of wideband RCS reduction.

Funding

National Natural Science Foundation of China (Grants Nos. 61331005, 61671467, 61501497); the Innovation Team of Shaanxi province (Grant No.2014KCT-05).